Chinese Chemical Letters 32 (2021) 291–298

Contents lists available at ScienceDirect

Chinese Chemical Letters

journal homepage: www.elsevier.com/locate/cclet

Review

# Transition metal carbides in electrocatalytic oxygen evolution reaction

Huaping Wang[a,b,1], Sheng Zhu[c,1], Jiwei Deng[a,*], Wenchao Zhang[d,*], Yuezhan Feng[e], Jianmin Ma[b,*]

[a] State Key Laboratory of High-Performance Complex Manufacturing, College of Mechanical and Electrical Engineering, Central South University, Changsha 410083, China
[b] School of Physics and Electronics, Hunan University, Changsha 410082, China
[c] Hunan Chengjin Elevator Parts Manufacturing Co., Ltd., Yueyang 414500, China
[d] Institute for Superconducting and Electronic Materials (ISEM), School of Mechanical, Materials, Mechatronics & Biomedical Engineering, Faculty of Engineering and Information Sciences, University of Wollongong, NSW 2500, Australia
[e] Key Laboratory of Materials Processing and Mold (Zhengzhou University), Ministry of Education, Zhengzhou University, Zhengzhou 450002, China

ARTICLE INFO

*Article history:*
Received 25 December 2019
Received in revised form 3 February 2020
Accepted 12 February 2020
Available online 13 February 2020

*Keywords:*
Transition metals
Carbides
Electrocatalysis
Oxygen evolution reaction
Performance

ABSTRACT

Oxygen evolution reaction (OER) is admitted to an important half reaction in water splitting for sustainable hydrogen production. The sluggish four-electron process is known to be the bottleneck for enhancing the efficiency of OER. In this regard, tremendous efforts have been devoted to developing effective catalysts for OER. In addition to Ir- or Ru-based oxides taken as the benchmark, transition metal carbides have attracted ever-increasing interest due to the high activity and stability as low-cost OER electrocatalysts. In this review, the transition metal carbides for water oxidation electrocatalysis concerning design strategies and synthesis are briefly summarized. Some typical applications for various carbides are also highlighted. Besides, the development trends and outlook are also discussed.


## 1. Introduction

In the last hundred years, human civilization has been developed to a striking distance due to the discovery and use of fossil energy. However, the overuse of fossil fuels has brought two issues: environmental pollution and energy crisis [1–4]. With the increasing demand for renewable and clean energy, developing new-generation energy storage and conversion devices as promising alternatives to traditional fossil fuels is crucial [5,6]. Hydrogen is known to be the optimal energy carrier due to its high energy density and accessibility from water electrolysis. Electrocatalytic water splitting is the best technology for hydrogen production owing to the non-polluting reactants and not any by-products, and it occurs as the reaction: $2H_2O \rightarrow 2H_2 + O_2$ [7,8]. Hence, hydrogen production from water electrolysis shows high promise [9].

Water splitting consists of two half reactions: the cathodic hydrogen evolution reaction (HER) and anodic oxygen evolution reaction (OER) [10–12]. The theoretical thermodynamic voltage for water splitting is 1.23 V. However, an additional overpotential is required to compensate the polarization-dependent loss. Generally, differentiated from the simple two-electron HER, OER needs to overwhelm the Gibbs energy barrier of four-step elementary reaction to proceed with the reaction thermodynamically [13,14]. So far, the application of water splitting in industry is mainly generated $H_2$ rather than $O_2$, thereby the sluggish four-step OER determines the efficiency of the overall water-splitting reaction. Therefore, in order to achieve the high efficiency of hydrogen production, it is paramount to develop competent catalysts, which can be used in the water splitting at an appropriate rate driven by a lower overpotential. Currently, noble metal oxides such as $IrO_2$ and $RuO_2$ have been employed as the benchmarking electrocatalysts for OER, but they suffer from the high price and poor stability, which severely impede their large-scale application [15]. Thus, tremendous efforts have been devoted to developing earth-abundant transition-metal-based electrocatalysts for OER, such as metal oxides [16], hydroxides [17,18], phosphates [19], chalcogenides [20], nitrides [21] and other metal-free materials [22].

Recently, transition metal carbides (TMCs) have attracted more attention in many catalytic fields due to the unique

* Corresponding authors at: Key Laboratory of Materials Processing and Mold (Zhengzhou University), Ministry of Education, Zhengzhou University, Zhengzhou 450002, China.
*E-mail addresses:* dengjw@csu.edu.cn (J. Deng), wenchao@uow.edu.au (W. Zhang), nanoelechem@hnu.edu.cn (J. Ma).
[1] These authors contributed equally to this work.

https://doi.org/10.1016/j.cclet.2020.02.018
1001-8417/

physicochemical properties, such as high stability, high electrical conductivity and high mechanical strength [23]. However, there are a few applications of carbides in electrocatalytic OER. On the one hand, carbides typically synthesized by the high temperature solid-state method, which made it difficult to large scale synthesize and application. On the other hand, their economic effects on industrial applications are not satisfied and too much energy is still being consumed in electrocatalytic water splitting. Excitedly, as the rapid development of nanotechnology, the investigations of carbides nanomaterials made tremendous advances in the past few decades [24,25]. By regulating structure and composition, TMCs nanomaterials are high performance electrocatalysts with extremely potent. Herein, we review the recent research of TMCs to achieve high activity and long-term stability OER electrocatalysts. The objective of this paper is to discuss the current challenges and provide a possible strategy for the future development of OER catalyst synthesis.

## 2. Design and construction of carbide-based electrocatalysts

Recently, carbide-based electrocatalysts with various morphologies, composition, and other additives have been aroused great interest owing to the satisfying disadvantages, such as the boosted reaction kinetics and stability. Numerous synthesis strategies have been explored to optimize nanostructures and compositions of carbide-based electrocatalysts (Table 1). In this section, we mainly focus on summarizing some typical synthetic methodology to obtain the high-efficiency carbide-based OER electrocatalysts.

### 2.1. Morphology control

By tuning the morphology of nanomaterials, a great deal of shapes such as nanospheres, nanorod, nanowire, nanosheet and so on, which could large activity surface area between catalysts and reactive species and more reaction sites for OER [26,27]. That is one of the most important factors for determining the performance of a catalyst.

To enlarge the active surface area, a series of morphologies have been well designed. For example, Abe *et al*. prepared $Ni_3C$ nanoparticles (NPs) with a size smaller than 10 nm. Due to the large surface areas, the $Ni_3C$ NPs exhibit excellent catalytic activity toward to the electrooxidation of $NaBH_4$ (Figs. 1a and b) [28]. Gao and colleagues have reported that successful synthesis of an effective cobalt-doping $Mo_2C$ nanowires (NWs) (Fig. 1c) [29]. The large surface in radial direction provides a large number of active sites, and the axial dimension advantageous to charge transfer and avoids material aggregation. As a result, the Co-doped $Mo_2C$ NWs showed high activity and excellent stability for electrocatalytic HER at both basic and acidic electrolytes. 2D nanomaterials represent a class of materials that show sheet-like structures, which possess the ultrathin thickness less than 5 nm with the width larger than 100 nm [26]. Except for NPs and NWs, nanosheets (NSs) such as 2D transition metal carbides (MXene) have shown greet competitive in energy storage [30–32]. For example, Barsoum *et al*. have reported that the large-scale synthesis of $Mo_2CTx$ flakes by etching of Ga from $Mo_2GaC$ (Fig. 1d) [33]. Due to the layered structure, large surface area, high conductivity, and mechanical properties, a large reversible capacity with 560 mAh/g has achieved under 0.4 A/g when the prepared materials were tested. Meanwhile, the $Mo_2CTx$ also showed excellent stability over 1000 cycles test. Vojvodic has also reported that the $Mo_2CTx$ as HER catalysts showed better activity and high stability in the acid electrolyte (Figs. 1e and f) [34].

**Table 1**
Summary of carbide-based electrocatalysts for OER with different structure.

| Synthesis strategies | Structures | OER performance ($\eta$ @10 mA/cm$^2$) |
|---|---|---|
| Control morphology | $Fe_3C$ NSs/Ni foam [63] | 262 mV |
| | $NiC_{0.2}$ NSs [81] | 228 mV |
| | $Mo_2CTx$ 3D microflowers [87] | 180 mV |
| Heterojunction | NiOx/$Ni_3C$ [73] | 330 mV |
| | Ni/$Ni_3C$ core/shell hierarchical nanospheres [74] | 350 mV |
| | $MoS_2/Mo_2C$ hybrid structure [83] | 280 mV |
| Modulation of component | Bimetallic Co/Mo carbide [47] | 260 mV |
| | $V_{0.28}Co_{0.72}C$/carbon nanofibers [70] | 240 mV |
| | Bimetallic $Mo_6Ni_6C$ [79] | 190 mV |
| Encapsulated | $Fe_3C$@NG [53] | 361 mV |
| | $Fe_3C$ NPs encapsulated in graphite [60] | 299 mV |
| | Ni/$Ni_3C$ encapsulated in NCNT [76] | 277 mV |

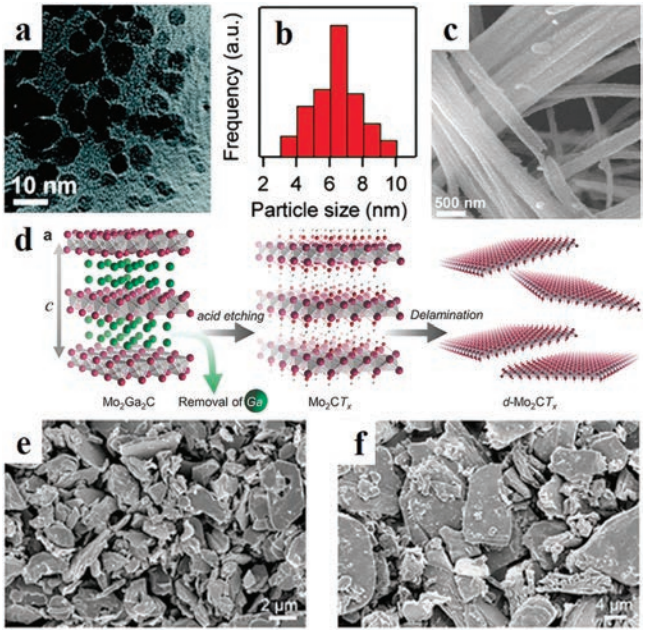


**Fig. 1.** (a) Transmission electron microscopy (TEM) image and (b) particle-size of $Ni_3C$ NPs. Reproduced with permission [28]. Copyright 2014, Royal Society of Chemistry. (c) Scanning electron microscopy (SEM) image of $Mo_2C$ NWs. Reproduced with permission [29]. Copyright 2016, Wiley. (d) Schematic of synthesis and delamination of $Mo_2CT_2$. Reproduced with permission [33]. Copyright 2016, Wiley. SEM images of (e) $Mo_2CTx$ and (f) $Ti_2CTx$. Reproduced with permission [34]. Copyright 2016, American Chemical Society.

### 2.2. Fabrication of heterojunctions

For the individual catalyst often possess an excellent performance, some with abundant active sites, some showed high conductivity. Heterojunctions could combine the individual property of individual catalysts which have been demonstrated to be efficient catalysis for chemical reactions.

Non-noble metal carbide is an economical and widely applicable electrocatalyst. However, the intrinsic activity of pure-phase carbides is usually poverty for electrocatalysis. Therefore, in order to enhance the intrinsic activity of non-noble metal carbide, fabrication of heterojunctions catalyst is an effective method. For example, the g-$C_3N_4$ is a fascinating polymer semiconductor material for photocatalysis with a lot of advantages such as high

chemical and thermal stability, excellent absorption properties, suitable band gap, easy fabrication, and low cost [35]. However, the sluggish reaction kinetics and fast recombination of the electron-hole pairs of g-$C_3N_4$ lead to a low quantum efficiency. Therefore, it is necessary to suppress recombination of electron-hole pairs of g-$C_3N_4$. By constructing nano-heterojunction, which could enhance the separation of electron-hole pairs and improve the surface reaction kinetics thus enhanced the photocatalytic performance. Li *et al*. have used $Ni_3C$ as cocatalysts to improve the performance of photocatalytic $H_2$ evolution over the g-$C_3N_4$ (Fig. 2a) [36]. Compare to the quantum yield of pure g-$C_3N_4$, that of $Ni_3C$ NPs on g-$C_3N_4$ achieved an incredible promotion. The result also showed that the $Ni_3C$/g-$C_3N_4$ possess excellent catalytic activity of photocatalytic $H_2$ evolution (Fig. 2b). In the photocatalytic $N_2$ reduction, the efficiency is too low due to the high bond energy of N≡N bond. Although various semiconductors have been investigated to $N_2$ reduction, unfortunately, the photoelectron was not provided enough energy to make the cleavage of N≡N bond. Lam and co-workers have designed an *in situ* grown $AnInS_2$ NPs@$Ti_3C_2$ NSs heterojunction (Fig. 2c), which can increase the energy of photoelectrons and promoting electronic accumulation on the surface of $Ti_3C_2$ [37]. The hybrids nanomaterial showed excellent photocatalytic $N_2$ reduction ability due to the optimized structure (Fig. 2d). All in all, the heterojunction effect on catalytic applications has important potential values [38].

Despite there are low-cost and efficient of TMCs heterojunction, it is relatively seldom applied as the catalyst for electrocatalytic water splitting.

### 2.3. Modulation of components

The surface electronic structure of catalysts is very important for the performance of the catalyst, which can control the adsorption of reactants and enhance the catalytic activity. The formation of multi-metallic structure is a common strategy to tune the property of electrocatalysts due to the interactions between different components, which is beneficial to tune the electronic structure and other physical and chemical properties of electrocatalysts then optimization the activities. This has been demonstrated by bimetallic [16,39–42] and trimetallic [27,43,44] for efficient electrocatalysis.

For example, Zhang's group prepared bimetallic carbide $Fe_2MoC$ NPs, which can adjust the electronic properties of iron carbide. As a result, the $Fe_2MoC$ has been verified to possess excellent performance (Figs. 3a and b) [45]. In addition, more bimetallic carbides have been reported for high activity used in electrocatalysts field [46,47]. Therefore, component control is an effective strategy to design high efficiency electrocatalyst.

In addition, doping is another effective way to boost the activity of catalysts. As a well know, by doping heteroatom into catalysts, the surface of catalysts is easier to turn to the oxidation state, then the energy barrier of OER could be effectively reduced and to boost catalytic performance [48–50]. Leonard has reported that the Fe-doped MoC NPs showed excellent HER catalytic performance [51]. The mechanism study demonstrates that Fe doping benefits to make lattice expansion and more electrons on catalyst surface around to Fermi level, which is the key factor to enhance the HER performance (Figs. 3c and d). Yan *et al*. has prepared Fe-doped $Ni_3C$ nanodots (NDs) based NSs [52]. By the introducing of Fe into the $Ni_3C$ NDs system, the as prepared material showed the best OER catalytic performance and the overpotential low to 275 mV at the current density of 10 mA/cm$^2$. The results indicating that doping is an effective strategy to boost the performance of OER electrocatalysis.

Up to date, multi-component TMCs have recently been successfully applied in the studies of electrocatalytic OER process. However, more research is still needed to improve the stability of these TMCs electrocatalysts.

### 2.4. Encapsulated in protective material

The stability of OER catalyst is also an important factor to determine the practical application. Therefore, substantial efforts also have been devoted to improving the stability of OER catalysis by tuning the structures. Among all the methods, the coating has been proven due to its superiority over the others in terms of enhancing stability, it is like that put catalyst in unique channel by graphene or other shell material. In this way, the metal catalyst can be protected and from damage in harsh conditions due to the shell can isolate the reaction molecules and catalyst.

Therefore, many different shell materials such as carbon nanotube, graphene and graphitic carbon nitride have been developed for the encapsulation. For example, the $Fe_3C$ NPs can be encapsulated in graphitic and dispersed on the N-doped graphene-like carbon sheets, the graphite layers around on the $Fe_3C$ NPs plays an important role in the significant stability of

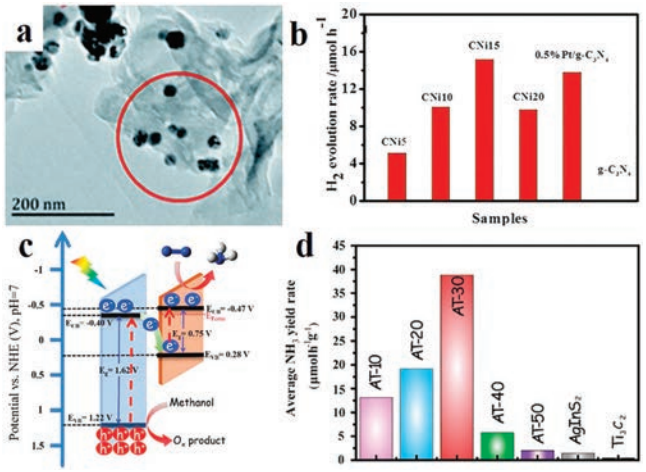


**Fig. 2.** (a) TEM image of CNi15 and (b) the average rates of $H_2$ evolution over different samples. Reproduced with permission [36]. Copyright 2013, Royal Society of Chemistry. (c) The energy band positions and (d) the comparison of $NH_3$ yield rate. Reproduced with permission [37]. Copyright 2019, Elsevier.

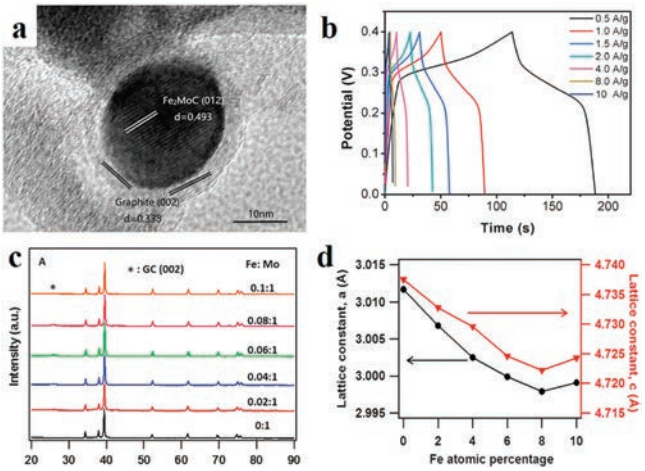


**Fig. 3.** (a) HRTEM image of $Fe_2MoC$ and (b) galvanostatic charge-discharge (GCD) curves of $Fe_2MoC$. Reproduced with permission [45]. Copyright 2018, Elsevier. (c) XRD patterns and (d) lattice parameter of $Mo_2C$ with different amount of Fe-doping. Reproduced with permission [51]. Copyright 2015, American Chemical Society.

$Fe_3C$@NG, which showed efficient electrocatalytic performance with high stability for ORR and OER (Figs. 4a-c) [53]. Carbon nanotube is an excellent material with high conductivity and high surface area. So, it can not only improve the stability, but also enhance the catalytic activity *via* encapsulating transition metal NPs into carbon nanotubes [54]. The transition metal NPs can be protected carbon layers, thus the catalysts possess superior stability (Figs. 4d and e). Significantly, due to the synergistic effects between core and carbon shell, the activity of the catalyst can also be enhanced. Wu *et al.* have reported carbon doped of N, O, S sheets-encapsulated $Co_9S_8$ nanomaterials and that material showed high activity and good stability in alkaline medium for OER. The excellent property is mainly due to the synergistic effects between the $Co_9S_8$ NPs and the multi-doped carbon in the materials [55].

Except for carbon materials, more 2D materials such as boron nitride, TM dichalcogenides and hydrotalcite can also be used for the encapsulation, which needs more studies to develop more excellent catalysts.

## 3. Metal carbides for electrocatalytic OER

As discussed above, carbides nanomaterials have great potential for electrocatalytic water oxidation. TMC has very excellent physical and chemical properties such as high electrical conductivity, good corrosion resistance, and high mechanical stability. Despite there are still difficult in large-scale synthesis and application, many achievements have been obtained of carbide nanomaterials. In this section, several typical carbides including iron, cobalt and nickel carbide electrocatalysts will be introduced for electrocatalytic OER in recent years.

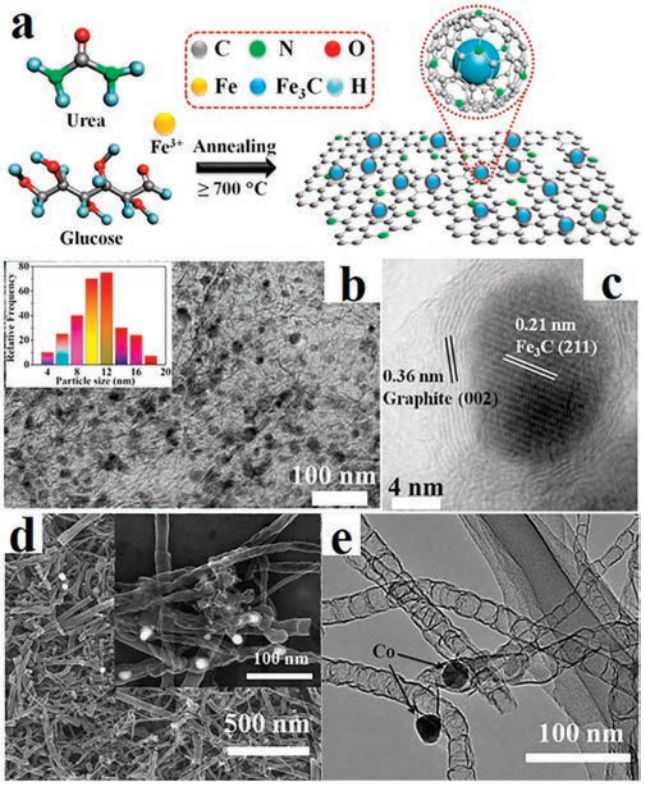


**Fig. 4.** (a) Scheme of the fabrication of $Fe_3C$@NG. (b) SEM and (c) TEM images of $Fe_3C$@NG. Reproduced with permission [53]. Copyright 2015, American Chemical Society. (d) SEM and (e) TEM images of Co/N-CNTs. Reproduced with permission [54]. Copyright 2016, Royal Society of Chemistry.

### 3.1. Iron carbides for electrocatalytic OER

Compared to noble metal materials, non-noble transition metals have many advantages such as low price, abundant resources, and low toxicity. In the recent study, it is found that the transition metal carbides have "platinum-like" electronic excellent catalytic performance. Iron is the most abundant metallic element on earth, so that the iron carbide has great application prospect for electrocatalytic OER.

However, iron carbide catalysts often suffer from poor electrical conductivity and poor stability, which reduced their catalytic performance. Therefore, the best way to address the above issues is to design composite material of iron carbide and conductive carrier. An efficient catalyst employed in the reaction should satisfy the demand of binding energies between reactive intermediates and catalytic surface [56]. Synergetic carbides/graphene-like carbon multicomponent materials have many active sites and high surface areas, which benefit to the transport of electrolyte ions and adsorption of reactants [57,58]. Encapsulated $Fe_3C$ NPs into porous carbon nitride [59], graphite [60], nitrogen functionalized carbon nanofibers [61] and N-doped carbon nanotubes [62], in which abundant porous can increase surface area and accelerating charge transfer thus to boost OER activity. For example, Lu and co-workers have designed $Fe_3C$ NSs@Ni foam (NF) nanocomposite by a one-step solvothermal and annealing method (Figs. 5a and b) [63]. The nanosheet structure of $Fe_3C$ can expose more active sites. Meanwhile, the unique three-dimensional structure of $Fe_3C$@NF made it have good electrical conductivity, large surface area, and more active sites. As a result, the $Fe_3C$@NF nanocomposite showed remarkable OER activity (Fig. 5c) amazing stability. Hierarchical structured of Fe/$Fe_3C$ NPs encapsulated by N-doped graphene also has been designed (Figs. 5d and e) [64]. The nanostructure showed high OER activity comparable to the $RuO_2$ catalysts (Fig. 5f).

To date, although have made remarkable achievements, the exploration of new iron carbide with higher OER activity remains a long way for the industrial application.

### 3.2. Cobalt carbides for electrocatalytic OER

Cobalt carbides ($Co_2C$ and $Co_3C$) have been used in Fischer-Tropsch (FT) synthesis reaction [65]. Although a few studies have discussed for OER, cobalt carbides still have suffered high overpotential due to the low intrinsic activity and poor stability in a harsh electrolyte [66].

Bimetallic materials considered to be very important candidates because of introduction of a second metal into single metal materials can adjust the electronic structure of active center and expose more active sites [45,46,67] Therefore, bimetallic carbide materials are also considered as a potential catalyst for OER [68,69]. Lan *et al.* have synthesized Co/Mo bimetallic carbide, which exhibits low overpotential of 260 mV, low Tafel slope and excellent stability (Figs. 6a and b) [47].

In addition, as an effective method to adjust the electronic structure of catalysts, heteroatom doping has been widely used in the synthesis of various catalysts. For example, Zhao *et al.* has reported a simple strategy of doping lower electronegative vanadium (V) into cobalt carbide, which results in most defects in the cobalt carbide lattice (Figs. 6c-e) [70]. Particularly, with the optimal doping amount, $V_{0.28}Co_{0.72}C$/carbon nanofibers (CNFs) display the best performance of electrocatalytic water splitting with the decomposition of 1.47 V at a current density of 10 mA/cm$^2$. The main reason for the significant increase of overall water splitting is that the electron density transfer from V to cobalt makes the cobalt as a local negative center. Chen *et al.* have reported a N,B-codoping $Co_3C$ catalyst, which showed high OER

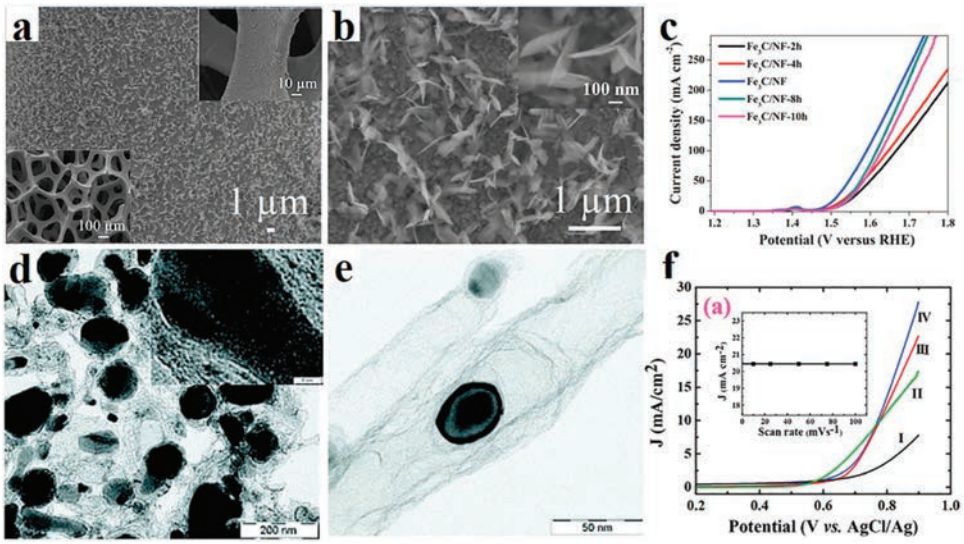


**Fig. 5.** (a, b) SEM images of $Fe_3C$ NSs/NF. (c) LSV of $Fe_3C$ NSs/NF prepared at different time in 1.0 mol/L KOH. Reproduced with permission [63]. Copyright 2019, Elsevier. (d, e) TEM images of Fe/$Fe_3C$ NPs/NG. (f) OER polarization curves of 20% Pt/C, commercial $RuO_2$ and Fe/$Fe_3C$ NPs/NG. Reproduced with permission [64]. Copyright 2016, Royal Society of Chemistry.

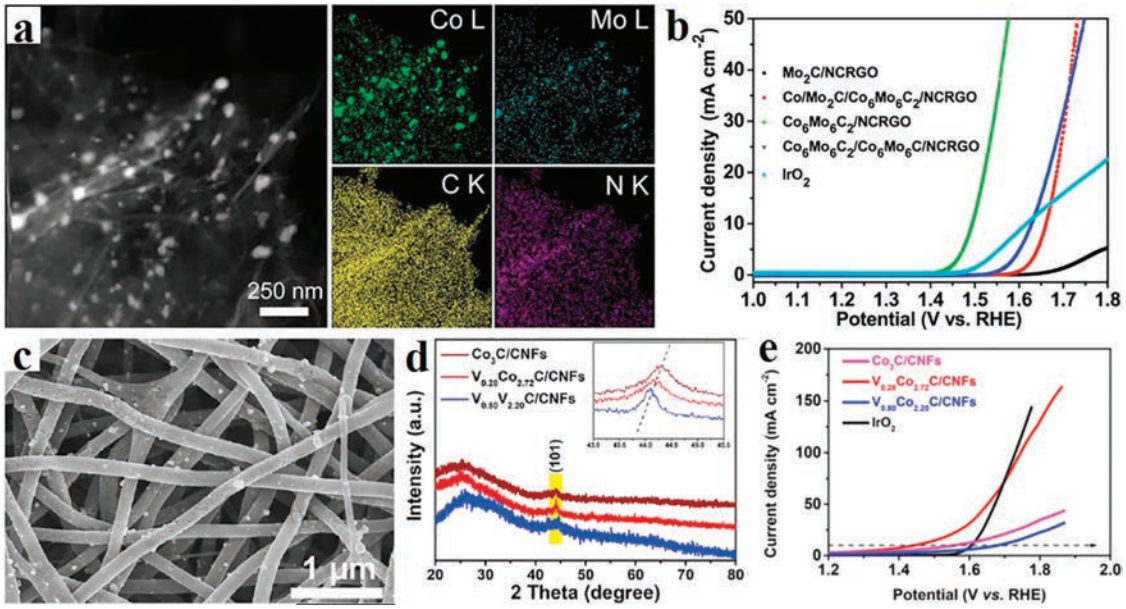


**Fig. 6.** (a) High-angle annular dark-field scanning TEM-EDS (HAADF-STEM) and element mapping of $Co_6Mo_6C_2$/NCRGO. (b) LSV curves of all samples and commercial $IrO_2$. Reproduced with permission [47]. Copyright 2017, American Chemical Society. (c) SEM images of $V_{0.28}Co_{2.72}C$/CNFs. (d) X-ray diffraction (XRD) and (e) polarization curves of different samples. Reproduced with permission [70]. Copyright 2019, American Chemical Society.

activity with the overpotential of 358 mV, as well as improved stabilities [71]. In addition, the porous structure is beneficial for the catalyst to obtain higher OER activity due to the high surface area and expose more active sites. For example, He's group prepared a hierarchical porous $Co_3C$/Co-N-C/G nanomaterial by a two-step method [72]. Due to more exposed active sites and the synergistic effects among all components, the as-prepared catalyst has shown high OER performance.

### 3.3. Nickel carbides for electrocatalytic OER

Nickel carbides are a promising electrocatalyst for OER due to the advantages of earth-abundance and superior electrical conductivity. $Ni_3C$ has attracted significant attention among various nickel carbide due to the excellent physicochemical properties such as high chemical stability and conductivity. For example, Xie *et al*. have synthesized $Ni_3C$/C composite as OER catalyst, which displayed excellent bifunction catalytic activity of HER and OER [73].

Optimization of electrocatalytic performance is very important for developing nickel carbides OER catalysts. Zheng's group reported the Ni/$Ni_3C$ core/shell hierarchical nanospheres. Benefit by this structure, more active site has exposed, which exhibited an outstanding electrocatalytic performance with a low of 350 mV at 10 mA/$cm^2$ for OER [74]. In order to improve the activity and stability of Ni/$Ni_3C$ catalyst, Zheng *et al*. have reported $Ni_3C$/N-doped carbon nanoflakes, in which the structure and composition can be controlled by charge the synthetic conditions [75]. Based on the composite nanostructure, $Ni_3C$/NC nanoflakes showed high electrocatalytic performance with a low overpotential

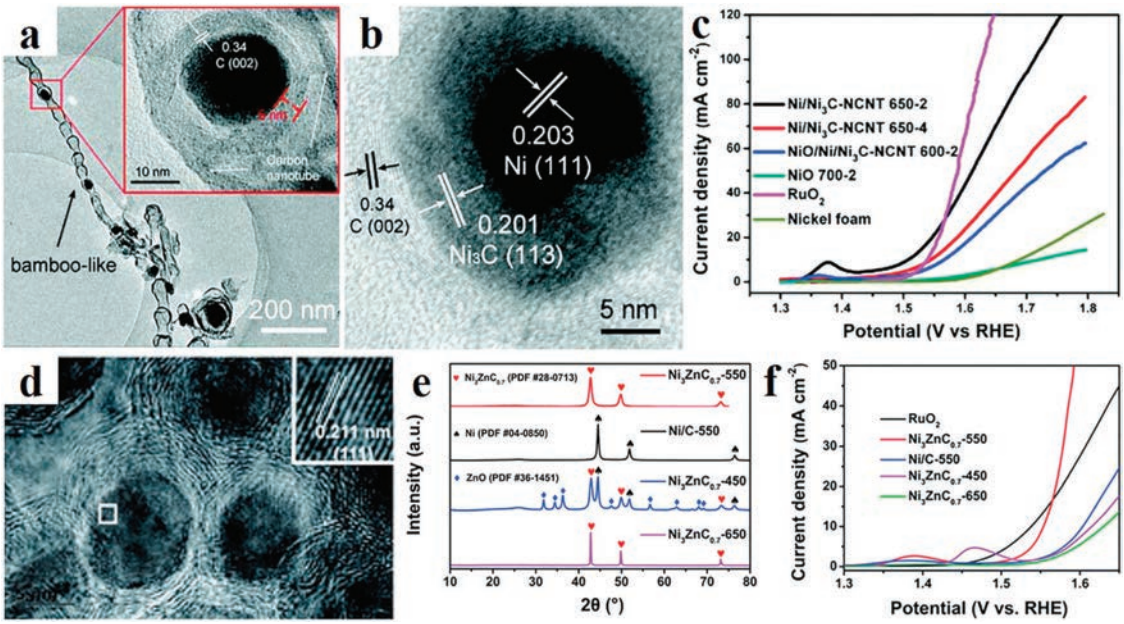


**Fig. 7.** (a, b) TEM and HR-TEM images of Ni/$Ni_3C$-NCNT. (c) LSV curves of Ni/$Ni_3C$-NCNT and contrast samples. Reproduced with permission [76]. Copyright 2019, Royal Society of Chemistry. (d) HR-TEM image of $Ni_3ZnC_{0.7}$. (e) XRD patterns and (f) LSV of different samples and commercial $RuO_2$. Reproduced with permission [77]. Copyright 2019, Elsevier.

of 309 mV. Yang *et al.* have fabricated N-doped carbon nanotubes encapsulated Ni/$Ni_3C$-NCNT material, in which $Ni_3C$ NPs was uniformly distributed in the wall of NCNT (Figs. 7a and b) [76]. Due to the unique composition and structure, the sample displayed improved OER catalytic activity with a low overpotential of 277 mV (Fig. 7c).

In electrocatalysis process, active center of catalyst with different valence states possesses different adsorption and desorption energies to intermediates. Therefore, rationally adjust the valence is an effective method to boost the performance of the catalyst. Introduction of metals with different electronegativity can effectively regulate the valence state of catalyst. For example,

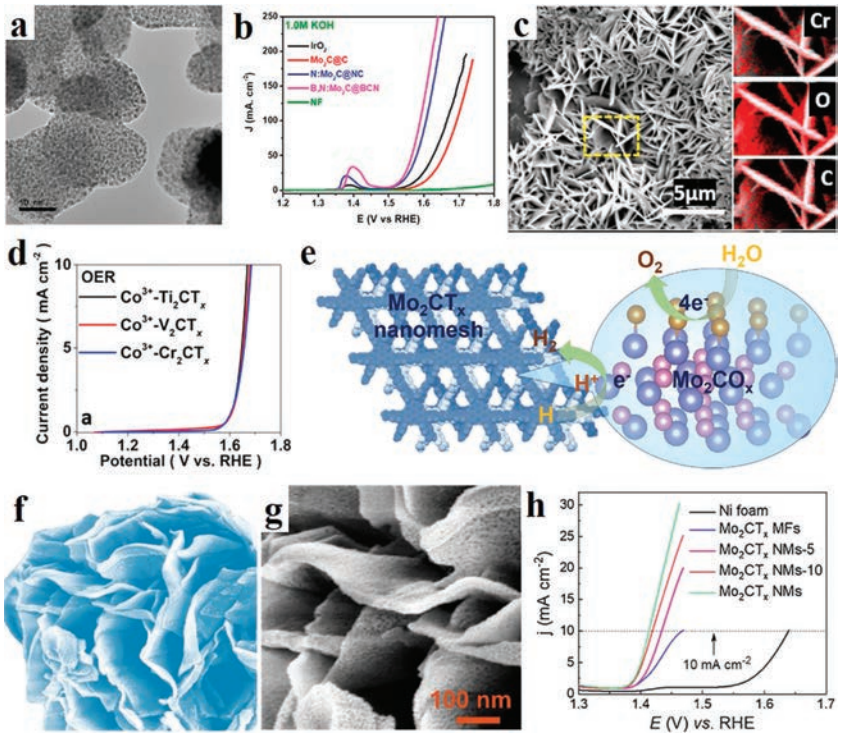


**Fig. 8.** (a) TEM image of $Mo_2C$ NPs imbedded in BCN. (b) OER polarization for different samples. Reproduced with permission [83]. Copyright 2018, American Chemical Society. (c) SEM image and elemental mapping of $Cr_2CTx$. (d) OER polarization for different samples. Reproduced with permission [86]. Copyright 2019, American Chemical Society. (e) Schematic illustration of the $Mo_2CTx$ for electrocatalytic OER. (f) Morphology simulation and (g) SEM image of the $Mo_2CTx$ MFs. (h) LSV curves of different samples. Reproduced with permission [87]. Copyright 2019, Elsevier.

the Zinc (Zn) can change the electronic property of bimetallic $Ni_3ZnC_{0.7}$ thus improved the OER activity (Figs. 7d-f) [77,78]. Yang *et al*. have reported that a high-valence metals "Molybdenum" (Mo) is introduced into nickel carbide to form bimetallic $Mo_6Ni_6C$ catalyst. In the catalytic process, high-valence $Mo^{6+}$ has incorporated with the Ni species and the carbon element insert into MoNi array at the atomic level, which effectively enhances the conductivity and exposes more active sites. So, the bimetallic $Mo_6Ni_6C$ showed amazing OER activity with an overpotential of 190 mV at a current density of 10 mA/cm$^2$ [79].

Heteroatom doping adjusts the electron structure of catalysts can also promote electron transfer thus enhance the catalytic property. For instance, Li *et al*. have synthesized the Co-doped $Ni_3C$/C compound material, which also showed outstanding OER catalytic performance compared to pure $Ni_3C$ [80]. In addition, high-index facets of catalyst usually have superior catalytic performance for OER. For this reason, Ma has prepared a high-index faceted $NiC_{0.2}$ NSs on Ni-coated copper foil [81]. The as-prepared catalyst also showed high catalytic activity and long-term stability for OER (overpotential of 228 mV at 10 mA/cm$^2$).

### *3.4. Other metal carbides for electrocatalytic OER*

Among all carbides, the molybdenum/tungsten (Mo/W) carbides used to be HER catalysts in the past studies. However, the metals of carbides are converted to OER-active species during the OER process [82]. Hence, there is still plenty of room for improvement to become high activity OER catalyst. For instance, the B, N-codoped $Mo_2C$ NPs encapsulated on B,N-codoped carbon network present excellent performances of HER and OER (Figs. 8a and b) [83]. Jeon's group proposed a $MoS_2/Mo_2C$ hybrid structure, in which the core-shell nanostructure showed excellent performance of ORR and OER with overpotential of 280 mV at 10 mA/cm$^2$, better than that of most other molybdenum carbide catalyst. The lattice strain in the core/shell structure is responsible for high ORR and OER activity [84]. Similarly, tungsten carbides have been widely used as HER catalyst due to the similar d-electronic structure like platinum. However, the $PbO_2$-WC composite has shown lower OER overpotential, indicating that WC has potential to be an efficient OER catalyst [85].

MXenes are promising materials for various energy storage devices and water splitting due to outstanding physicochemical properties such as high electrical conductivity, porosity, and stability. For example, Hao *et al*. have proposed an electrochemical etching method to synthesis MXenes (Fig. 8c) [86]. When the as-prepared material was employed to water oxidation (Fig. 8d), the catalytic performance is comparable to commercial $IrO_2$. Due to the limitation of traditional synthesis method, the prepared 2D MXenes are dense and tend to stack together, which leads to a poor mass transfer and active sites for electrocatalytic water splitting. One approach to solve this problem is to assemble 2D MXenes into 3D structure. Wang *et al*. develop a pyrolysis method and surface engineering to prepare molybdenum carbide ($Mo_2CTx$) 3D microflowers (MFs) structure (Fig. 8e) [87]. Benefit from the outstanding structural (Figs. 8f and g), such $Mo_2CTx$ showed ultrahigh electrocatalytic OER activity with an overpotential of only 180 mV to achieve a current density of 10 mA/cm$^2$ (Fig. 8h). In addition, MXenes are potential carrier materials due to high surface area and electronegative surfaces, which may charge the electronic structure of the multicomponent catalyst thus most catalytic performance. For example, the MXenes can carry CoBDC MOF [88] or FeNi-LDH [89]. As a result, both MOF/$Ti_3C_2Tx$ and FeNi-LDH/$Ti_3C_2$-MXene can exhibit superior activity and durability for OER. Manganese (Mn) carbide catalysts has also investigated for OER. For example, Streb's group synthesized metal oxides/carbides-CNT hybrid material with Mn/V oxide as a precursor [90].

## 4. Summary and outlook

In this review, we have summarized the development of transition metal carbides OER electrocatalysts, such as Fe-, Co-, Ni-, Mo-, W-based carbides, many strategies have been deployed to improve electrocatalytic performance for electrocatalytic OER, including morphology control, heterojunction, component control, and coating of conductive substrates. Although the transition metal carbides show high electron conductivity, desirable catalytic activity, and decent stability after the optimization of structure and composition, the performance of metal carbide is still not up to the level of the best catalyst such as layered double hydroxide. So, some problems should be solved as follows:

(1) The current synthesis methods for metal carbides possess obvious disadvantages which limit their large-scale application. With the development of materials science, it must develop a simple, efficient and widely used synthesis method to prepare transition metal carbide nanostructures.

(2) In the past design, metal carbide particles are usually spherical particles. For the morphologies design, this is very single. By designing carbide with special shape like cube, octahedral and polyhedron, we will further reveal the effect of crystal surface of metal carbide for electrocatalytic OER performance. So that to guide us to synthesize more efficient TMCs catalyst.

(3) It is remarkable that high-index facets of catalyst usually have superior catalytic performance for OER. Although various structures and morphologies have been designed, the design of high index carbide materials is rare. If we can design more carbide with a high index surface, it is hopeful to further improve the catalytic performance of carbide materials for OER.

As a great potential catalyst, metal carbides will have more applications in the future.

## Declaration of competing interest

The authors declare no conflict of interest.

## Acknowledgments

This work was supported by the National Natural Science Foundation of China (Nos. 51302079, 51702138), the Natural Science Foundation of Hunan Province (No. 2017JJ1008), and the Key Research and Development Program of Hunan Province of China (No. 2018GK2031).

## References

[1] Y. Wu, X. Liu, D. Han, et al., Nat. Commun. 9 (2018) 1425.
[2] L. Wang, X. Zheng, L. Chen, Y. Xiong, H. Xu, Angew. Chem. Int. Ed. 57 (2018) 3454–3458.
[3] J. Liao, W. Ni, C. Wang, J. Ma, Chem. Eng. J. 391 (2020) 123489.
[4] Z. Wei, B. Ding, H. Dou, et al., Chin. Chem. Lett. 30 (2019) 2110–2122.
[5] B. Xu, S. Qi, F. Li, et al., Chin. Chem. Lett. 31 (2020) 217–222.
[6] X. Xie, S. Qi, D. Wu, et al., Chin. Chem. Lett. 31 (2020) 223–226.
[7] M.E.G. Lyons, R.L. Doyle, D. Fernandez, et al., Electrochem. commun. 45 (2014) 56–59.
[8] J. Feng, F. Lv, W. Zhang, et al., Adv. Mater. 29 (2017) 1703798.
[9] Y. Chen, S. Xu, Y. Li, et al., Adv. Energy Mater. 7 (2017) 1700482.
[10] J. Liu, Y. Zheng, Y. Jiao, et al., Small 14 (2018) e1704073.
[11] Y. Yang, Y. Tang, H. Jiang, et al., Chin. Chem. Lett. 30 (2019) 2089–2109.
[12] Y. Yang, M. Wu, X. Zhu, et al., Chin. Chem. Lett. 30 (2019) 2065–2088.
[13] Y. Ding, Y. Niu, J. Yang, et al., Small 12 (2016) 5414–5421.
[14] J.K. Hurst, Science 328 (2010) 315–316.
[15] F. Hu, S. Zhu, S. Chen, et al., Adv. Mater. 29 (2017) 1606570.
[16] S.V. Devaguptapu, S. Hwang, S. Karakalos, et al., ACS Appl. Mater. Inter. 9 (2017) 44567–44578.
[17] M.S. Burke, M.G. Kast, L. Trotochaud, A.M. Smith, S.W. Boettcher, J. Am. Chem. Soc. 137 (2015) 3638–3648.
[18] N. Hussain, W. Yang, J. Dou, et al., J. Mater. Chem. A 7 (2019) 9656–9664.
[19] H. Duan, D. Li, Y. Tang, et al., J. Am. Chem. Soc. 139 (2017) 5494–5502.
[20] J. Yin, Y. Li, F. Lv, et al., Adv. Mater. 29 (2017) 1704681.

[21] Z. Chen, Y. Song, J. Cai, et al., Angew. Chem. Int. Ed. 57 (2018) 5076–5080.
[22] X. Cui, P. Ren, D. Deng, J. Deng, X. Bao, Energy Environ. Sci. 9 (2016) 123–129.
[23] S.R. Chemler, M.T. Bovino, ACS Catal. 3 (2013) 1076–1091.
[24] K. Guo, D. Rau, L. Toffoletti, et al., Chem. Mater. 24 (2012) 4600–4606.
[25] Y. Hu, J.O. Jensen, W. Zhang, et al., Angew. Chem. Int. Ed. 53 (2014) 3675–3679.
[26] C. Tan, X. Cao, X.J. Wu, et al., Chem. Rev. 117 (2017) 6225–6331.
[27] Y. Pi, Q. Shao, P. Wang, et al., Angew. Chem. 56 (2017) 4502–4506.
[28] N.A. Fadil, G. Saravanan, G.V. Ramesh, et al., Chem. Commun. 50 (2014) 6451–6453.
[29] H. Lin, N. Liu, Z. Shi, et al., Adv. Funct. Mater. 26 (2016) 5590–5598.
[30] B. Xu, M. Zhu, W. Zhang, et al., Adv. Mater. 28 (2016) 3333–3339.
[31] X. Zhang, Z. Zhang, J. Li, et al., J. Mater. Chem. A 5 (2017) 12899–12903.
[32] H. Jiang, Z. Wang, Q. Yang, et al., Nano-Micro Lett. 11 (2019) 31.
[33] J. Halim, S. Kota, M.R. Lukatskaya, et al., Adv. Funct. Mater. 26 (2016) 3118–3127.
[34] Z.W. Seh, K.D. Fredrickson, B. Anasori, et al., ACS Energy Lett. 1 (2016) 589–594.
[35] X. Wang, K. Maeda, A. Thomas, et al., Nat. Mater. 8 (2009) 76–80.
[36] K. He, J. Xie, Z.Q. Liu, et al., J. Mater. Chem. A 6 (2018) 13110–13122.
[37] J. Qin, X. Hu, X. Li, et al., Nano Energy 61 (2019) 27–35.
[38] J. Su, G.D. Li, X.H. Li, J.S. Chen, Adv. Sci. 6 (2019)1801702.
[39] J. Ding, Q. Shao, Y. Feng, X. Huang, Nano Energy 47 (2018) 1–7.
[40] D. Zhao, K. Jiang, Y. Pi, X. Huang, ChemCatChem 9 (2017) 84–88.
[41] Y. Zhang, Q. Shao, S. Long, X. Huang, Nano Energy 45 (2018) 448–455.
[42] M. Yao, N. Wang, W. Hu, S. Komarneni, Appl. Catal. B: Environ. 233 (2018) 226–233.
[43] L. Jin, H. Xu, C. Chen, et al., ACS Appl. Mater. Inter. (2019) 42123–42130.
[44] B. Li, Y. Chen, Y. Zong, et al., Environ. Microbiol. 21 (2019) 1124–1139.
[45] X. Hao, J. Bi, W. Wang, et al., Ceram. Int. 44 (2018) 21874–21881.
[46] Z. Yan, M. Zhang, J. Xie, P.K. Shen, J. Power, Sources 295 (2015) 156–161.
[47] Y.J. Tang, C.H. Liu, W. Huang, et al., ACS Appl. Mater. Inter. 9 (2017) 16977–16985.
[48] X. Xu, C. Su, W. Zhou, et al., Adv. Sci. 3 (2016) 1500187.
[49] Y. Duan, S. Sun, S. Xi, et al., Chem. Mater. 29 (2017) 10534–10541.
[50] Y. Zhou, M. Luo, Z. Zhang, et al., Appl. Surf. Sci. 448 (2018) 9–15.
[51] C. Wan, B.M. Leonard, Chem. Mater. 27 (2015) 4281–4288.
[52] H. Fan, H. Yu, Y. Zhang, et al., Angew. Chem. Int. Ed. 56 (2017) 12566–12570.
[53] H. Jiang, Y. Yao, Y. Zhu, et al., ACS Appl. Mater. Inter. 7 (2015) 21511–21520.
[54] Y. Liu, H. Jiang, Y. Zhu, X. Yang, C. Li, J Mater. Chem. A 4 (2016) 1694–1701.
[55] S. Huang, Y. Meng, S. He, et al., Adv. Funct. Mater. 27 (2017)1606585.
[56] C.C. Yang, S.F. Zai, Y.T. Zhou, L. Du, Q. Jiang, Adv. Funct. Mater. (2019) 1901949.
[57] Z. Li, Q. Gao, X. Liang, et al., Carbon 150 (2019) 93–100.
[58] Y. Tian, L. Xu, J. Qian, et al., Carbon 146 (2019) 763–771.
[59] L. Wei, H. Sun, T. Yang, et al., Appl. Surf. Sci. 439 (2018) 439–446.
[60] Y. Zhang, J. Zai, K. He, X. Qian, Chem. Commun. 54 (2018) 3158–3161.
[61] Y. Zhao, J. Zhang, X. Guo, et al., J. Mater. Chem. A 5 (2017) 19672–19679.
[62] X. Chen, J. Xu, H. Chai, et al., J. Electroanal. Chem. 838 (2019) 16–22.
[63] S. Zhu, J. Lei, L. Zhang, L. Lu, Int. J. Hydrogen Energy 44 (2019) 16507–16515.
[64] B.K. Barman, K.K. Nanda, Green Chem. 18 (2016) 427–432.
[65] J.C. Mohandas, M.K. Gnanamani, G. Jacobs, et al., ACS Catal. 1 (2011) 1581–1588.
[66] J.H. Kim, K. Kawashima, B.R. Wygant, et al., ACS Appl. Energy. Mater. 1 (2018) 5145–5150.
[67] Y. Xu, A. Tsou, Y. Fu, et al., Electrochim. Acta 174 (2015) 551–556.
[68] J. Su, G. Xia, R. Li, et al., J. Mater. Chem. A 4 (2016) 9204–9212.
[69] Z. Yu, Y. Bai, S. Zhang, et al., ACS Appl. Mater. Inter. 10 (2018) 6245–6252.
[70] S. Zhang, G. Gao, J. Hao, et al., ACS Appl. Mater. Inter. (2019) 43261–43269.
[71] X. Ma, K. Li, X. Zhang, et al., J. Mater. Chem. A 7 (2019) 14904–14915.
[72] X.X. Ma, X.Q. He, T. Asefa, Electrochim. Acta 257 (2017) 40–48.
[73] K. Xu, H. Ding, H. Lv, et al., Adv. Mater. 28 (2016) 3326–3332.
[74] Q. Qin, J. Hao, W. Zheng, ACS Appl. Mater. Inter. 10 (2018) 17827–17834.
[75] J. Hao, G. Zhang, Y. Zheng, et al., Electrochim. Acta 320 (2019) 134631.
[76] T. Dong, X. Zhang, Y. Cao, H.S. Chen, P. Yang, Inorg. Chem. Front. 6 (2019) 1073–1080.
[77] R. Li, X. Li, D. Yu, et al., Carbon 148 (2019) 496–503.
[78] Y. Wang, W. Wu, Y. Rao, et al., J. Mater. Chem. A 5 (2017) 6170–6177.
[79] M.Y. Zu, C. Wang, L. Zhang, L.R. Zheng, H.G. Yang, Mater. Horiz. 6 (2019) 115–121.
[80] X. Jia, M. Wang, G. Liu, et al., Int. J. Hydrogen Energy 44 (2019) 24572–24579.
[81] H. Yang, S. Luo, X. Li, et al., J. Mater. Chem. A 4 (2016) 18499–18508.
[82] J. Jiang, Q. Liu, C. Zeng, L. Ai, J. Mater. Chem. A 5 (2017) 16929–16935.
[83] M.A.R. Anjum, M.H. Lee, J.S. Lee, ACS Catal. 8 (2018) 8296–8305.
[84] A.P. Tiwari, Y. Yoon, T.G. Novak, et al., Adv. Mater. Inter. (2019) 1900948.
[85] S. He, Int. J. Electrochem. Sci. (2019) 4397–4408.
[86] S.Y. Pang, Y.T. Wong, S. Yuan, et al., J. Am. Chem. Soc. 141 (2019) 9610–9616.
[87] Z. Kou, L. Zhang, Y. Ma, et al., Appl. Catal. B: Environ. 243 (2019) 678–685.
[88] L. Zhao, B. Dong, S. Li, et al., ACS Nano 11 (2017) 5800–5807.
[89] M. Yu, S. Zhou, Z. Wang, J. Zhao, J. Qiu, Nano Energy 44 (2018) 181–190.
[90] X. Xing, R. Liu, K. Cao, U. Kaiser, C. Streb, Chem 25 (2019) 11098–11104.